Fretting wear study of surface modified Ni–Ti shape memory alloy

L. TAN
Materials Science Program, University of Wisconsin, Madison, 53706, USA
W. C. CRONE, K. SRIDHARAN
Department of Engineering Physics, University of Wisconsin, Madison, 53706, USA

A combination of shape memory characteristics, pseudoelasticity, and good damping properties make near-equiatomic nickel–titanium (Ni–Ti) alloy a desirable candidate material for certain biomedical device applications. The alloy has moderately good wear resistance, however, further improvements in this regard would be beneficial from the perspective of reducing wear debris generation, improving biocompatibility, and preventing failure during service. Fretting wear tests of Ni–Ti in both austenitic and martensitic microstructural conditions were performed with the goal of simulating wear which medical devices such as stents may experience during surgical implantation or service. The tests were performed using a stainless steel stylus counter-wearing surface under dry conditions and also with artificial plasma containing 80 g/L albumen protein as lubricant. Additionally, the research explores the feasibility of surface modification by sequential ion implantation with argon and oxygen to enhance the wear characteristics of the Ni–Ti alloy. Each of these implantations was performed to a dose of 3×10^{17} atom/cm^2 and an energy of 50 kV, using the plasma source ion implantation process. Improvements in wear resistance were observed for the austenitic samples implanted with argon and oxygen. Ion implantation with argon also reduced the surface Ni content with respect to Ti due to differential sputtering rates of the two elements, an effect that points toward improved biocompatibility.

Introduction

The Nickel–Titanium (Ni–Ti) shape memory alloy (nitinol) has been widely employed in the medical device industry because of the material's ability to exhibit predictable thermally activated shape changes and constant transformation stress over a wide strain range [1]. The alloy has been used for making orthodontic dental arch wires and medical guide wires for diagnostic and therapeutic catheters for many years. More recently, Ni–Ti has been used in endovascular stents to provide a self-expanding mechanical superstructure that is collapsed into a catheter and transported in compact form for more precise and less invasive implantation [2]. There are several characteristics which make Ni–Ti extremely attractive for use in medical devices. The material has generally good biocompatibility and, due to a reversible transformation between austenite and martensite crystal structures, devices made with this alloy can be pseudoelastically or thermally deployed. Additionally, Ni–Ti alloy has been shown to exhibit good resistance to wear, corrosion, and fatigue, which are important properties for biomedical device applications [3–6].

Although Ni–Ti is being used in a number of implantable medical devices, questions still remain regarding this material's long-term biocompatibility [7–8]. In studies of the *in vivo* use of Ni–Ti in orthodontic devices, several cases of severe inflammatory reactions resulting in contact dermatitis and oral lesions have been reported [9–11]. In Ni–Ti orthopedic applications cytotoxic effects were observed on osteoblast cells, which inhibited bone remodeling [12]. Furthermore, significant variations in the biocompatibility of this material have been reported depending on the surface treatment and sterilization method used prior to implantation [1, 13–14]. Such findings have prohibited the use of this alloy in specific acute cases and decreased the level of confidence in the biocompatibility originally attributed to this material.

The reduced biocompatibility of Ni–Ti is in large part due to the toxicity of nickel, which produces severe inflammatory reaction [7–8]. In contrast, Ti imparts biocompatibility by forming a tenacious film of titanium-dioxide, TiO_2, on the alloy surface. TiO_2 is inert to the human body and acts as a barrier to the release of metal ions, in particular the Ni^{+2} ions. It has been speculated that despite the presence of this oxide film, some release of Ni^{+2} is inevitable due to the presence of Ni-domains

in the alloy where the coverage by the oxide film may be inadequate [15]. In any event, it is clear that the preservation of the TiO_2 layer is crucial to the biocompatibility of the alloy, and any disruption of the oxide film due to mechanical attrition can reduce its biocompatibility. This would be a source of concern in the stent application for instance, where the cardiologist is often faced with the repair of a long section of a vessel or a branched vessel, requiring the use of multiple stents which may overlap or adjoin leading to the possibility of wear [16]. Relative cyclic motion between stents can occur as a result of pulsation in the vasculature or physical movement of the body. These wear processes may not only disrupt the protective oxide film, but can also result in the generation of wear debris, further increasing the risks for immunologic response.

The present study was undertaken to examine the feasibility of the non-line-of-sight ion implantation technique, plasma source ion implantation, to enhance the fretting wear resistance of Ni–Ti alloy. Ion implantation is especially suited for the surface modification of Ni–Ti alloy, because it is carried out at near-room temperature and therefore does not significantly alter the microstructure and bulk properties of the alloy. Additionally, because the modified surface layer is compositionally graded, there is no distinct interface between the surface modified layer and the bulk material. This is a critical point because the surface layer must be able to undergo large reversible strains when the bulk material transforms. Deposition of an overlay coating would lead to the possibility of interfacial delamination and debris generation due to the large reversible strains exhibited by the material in its use in biomedical applications. The depth of the ion implanted layer depends upon the acceleration energy, and is on the order of a few hundred nanometers.

Limited studies using conventional beam-line ion implantation of nitrogen into Ni–Ti have demonstrated an improvement in surface hardness and wear resistance, enhancement of surface passivation, and reduced friction coefficient for this alloy [17–19]. Plasma source ion implantation differs from the conventional beam-line ion implantation used in these studies, in that the parts to be treated are placed in the plasma source and pulse biased negatively so that the ions impinge on the part's surface normally. The conformality of the ions around the part's surface confers the non-line-of-sight nature to this process which may make this process a relatively cost-effective approach for the ion implantation of three-dimensional parts [20–21].

Experimental procedure

The material used in this work was a commercial Ti–50.8 at % Ni alloy in sheet form (0.81 mm in thickness) procured from Shape Memory Applications, Inc. in the flat annealed condition. The sheet was cut into $5 \times 10\,mm^2$ of flat samples by electro-discharge machining (EDM), chemically etched with an $1HF + 4HNO_3 + 5H_2O$ solution, and mechanically polished using SiC paper in successive grades from 240 to 1000 grit followed by a final polish with a 1 micron diamond lapping compound.

Nickel–titanium is a material with shape memory and pseudoelastic properties, which can transform between a martensitic phase, stable at low temperatures and high stress, and an austenitic phase, stable at high temperatures and low stress. Transformation from austenite to martensite can be induced by lowering the temperature of the material through the martensite start (M_s) and martensite finish (M_f) transformation temperatures. Conversely, transformation from martensite to austenite occurs upon heating through the austenite start (A_s) and austenite finish (A_f) transformation temperatures. The temperatures at which these transformations occur can be adjusted by changing the material composition or adjusting the heat treatment process. Transformation from austenite to martensite can also be induced in the material above the A_f temperature by loading the material to exceed the transformation stress, σ_T. The transformation stress is a temperature dependent material property which increases linearly with increasing temperature. The reverse transformation from martensite to austenite is observed when the material is unloaded.

In order to produce material in the austenitic form at room temperature, the as-received alloy was aged at 300 °C for 40 min, followed by quenching in water at room temperature. To obtain material in the martensitic structure at room temperature, the samples were aged at 500 °C for 10 min followed by cooling in a furnace. The critical temperatures of the transformations were determined by differential scanning calorimetry (DSC). The A_f temperature was determined to be 16 °C for the austenitic samples and 40 °C for the martensitic samples, thus they have the phase structure indicated by their names at room temperature.

The samples were ion implanted using the non-line-of-sight of plasma source ion implantation process, while the remaining were saved as control samples. As preparation for ion implantation, the samples were initially cleaned ultra-sonically in acetone, and, once in the plasma source ion implantation chamber, the samples were sputter-cleaned with energetic ions from an argon plasma at 6.5 kV to remove any residual surface contaminants. The surface modification process of involved argon ion implantation followed sequentially with oxygen ion implantation. Each of these implantations was carried out at 50 kV target voltage and an incident ion dose of 3×10^{17} atoms/cm^2.

DSC on control (unimplanted) and ion implanted samples identified a 5 °C decrease in transformation temperatures after ion implantation due to mild heating during the ion implantation process. This heating during ion implantation did not inhibit the shape memory and pseudoelastic properties of Ni–Ti as confirmed by cyclic mechanical testing of Ni–Ti wires reported by the authors in a previous study [22].

The near-surface hardness of the samples was measured using a low-load microhardness tester at loads of 10 g and 5 g. Owing to the small size-scale of the indentation, these measurements were made on well-polished flats, and at least ten measurements were made per sample per test load. A standard Knoop diamond indenter was employed as it provides for a higher

resolution of hardness as a function of depth compared to the Vickers indenter. Furthermore, with the rhombohedral shape of the Knoop indenter and the high diagonal-to-depth ratio (30 : 1), changes in indentation shape upon unloading due to elastic and pseudoelastic recovery can be held to a minimum [23].

Fretting wear tests of ion implanted and control samples were conducted using an in-house built-fretting wear tester. In this system, a spherical stylus is impressed on the test flat sample with a specific load and oscillated over short distances (10–500 μm) at high frequencies (10–100 Hz). The machine uses an electromagnetic actuator under closed-loop control to provide this kind of high frequency, oscillatory motion. The design of the machine allows for the measurement of relative friction at the resonant frequency during the progress of the fretting wear test [24]. The machine is particularly useful for testing surface modified materials, where information relating to changing wear mechanisms may be continuously obtained as wear proceeds through the modified layer. A schematic illustration stylus-sample configuration for fretting wear testing is shown in Fig. 1.

The present study was conducted using a 1/8 inch diameter stainless steel (AISI grade 316) stylus and an applied force of 0.2 N. This stylus material was chosen because of its widespread use in medical device applications. The tests were carried out for 10 000 cycles, with the stylus oscillating at a frequency of 20 Hz over a linear displacement of 100 μm. The tests were performed both in dry condition in ambient air, as well as in the lubricated condition using artificial plasma with 80 g/L albumen protein as the lubricant [25]. The composition of this solution is summarized in Table 1. The wear scar was measured using an alpha-step profilometer and examined with a scanning electron microscope (SEM).

TABLE I Composition of the artificial plasma lubricant used in the fretting wear tests

Component	Concentration (g/L)
NaCl	6.800
$CaCl_2$	0.264
KCl	0.400
$MgSO_4$	0.205
$NaHCO_3$	2.200
Na_2HPO_4	0.126
NaH_2PO_4	0.0299
Albumen protein	80

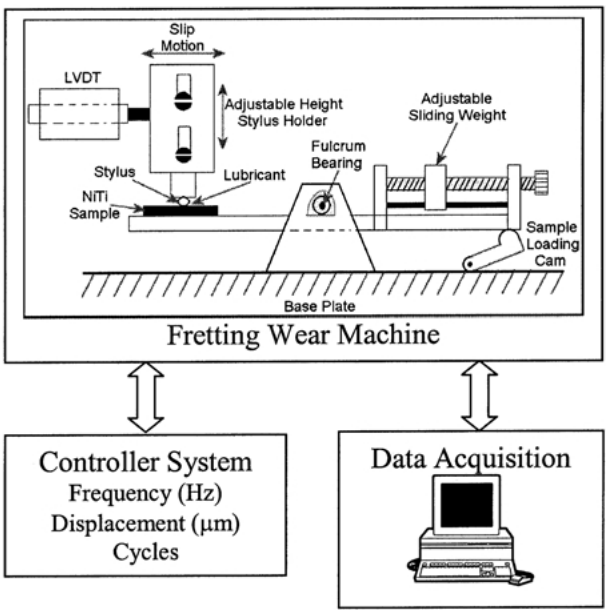

Figure 1 Schematic illustration of the stylus-sample configuration in the fretting wear test employed in the present study.

Experimental results

Fig. 2 shows the surface composition for the Ni–Ti alloy in the austenitic condition without surface modification (control) and after sequential ion implantation with argon and oxygen (Ar + O implanted). The high oxygen at the surface is indicative of the presence of TiO_2 film, which imparts biocompatibility to the alloy. During argon bombardment, the Ni content in the near-surface regions is reduced as a result of differential sputtering between Ni and Ti [22]. For the ion energies used in this study (50 kV), Ni sputters at a rate four times greater than Ti [26]. Fig. 2 indicates that nickel is absent from the material surface after plasma source ion implantation (PSII) treatment with argon and oxygen. Because Ni is toxic to the body, this decreased surface Ni content is speculated to be favorable to biocompatibility. Auger composition vs. depth profiles were obtained up to depths of about 500 nm. These results show evidence of some mixing of the surface oxide film deeper into the surface as a result of energetic ion bombardment. For samples implanted with oxygen, a deeper oxygen profile extending to about 200 nm was observed. Because of the strong affinity of Ti for oxygen, it is speculated that most of this oxygen is chemically bonded as TiO_2 and of TiO. Some carbon is also present on the surface of the sample prior to ion implantation and mixed into the surface of the material with ion bombardment. Qualitative examination of the broad-scan from Auger

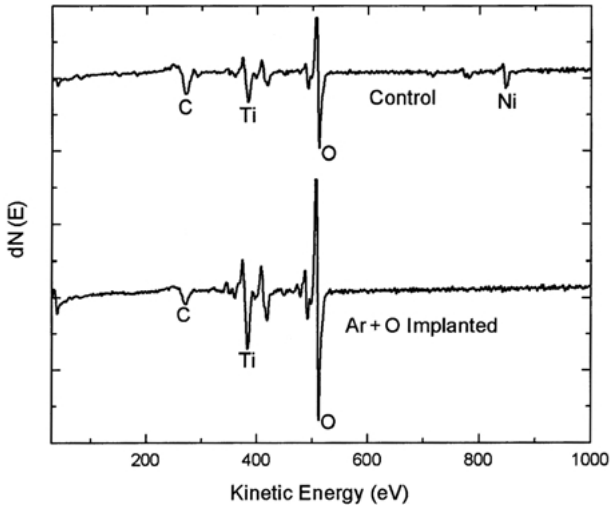

Figure 2 Auger composition profile for the unmodified Ni–Ti alloy, after sequential argon and oxygen ion implantation. Nickel is absent from the material surface after PSII treatment.

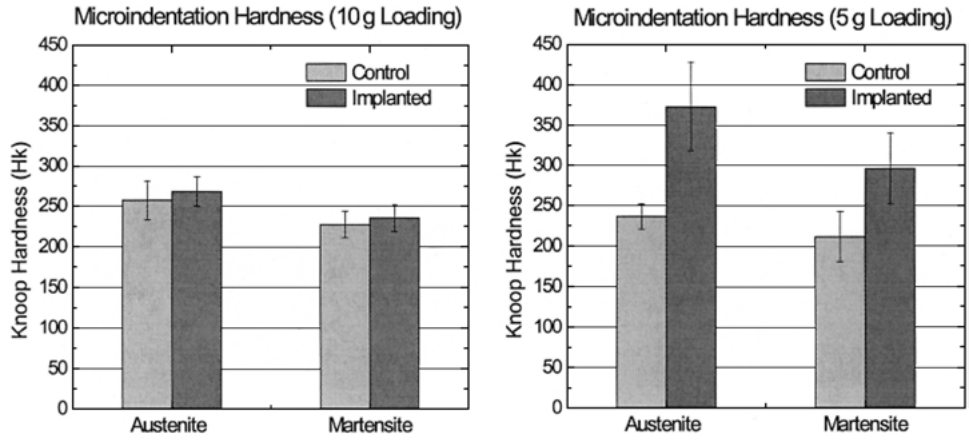

Figure 3 Microindentation hardness of austenite and martensitic samples under 10 g and 5 g loads.

analysis indicated that the carbon is bound as a carbide, which would act to further increase the hardness of the modified layer.

Results of low-load microhardness measurements are summarized in Fig. 3. Greater improvements in hardness are recorded at the lower load (5 g) because the indentation depth is on the order of the thickness of the modified layer. In reality, however, even at low loads, the indentation depth is influenced by the more compliant bulk material beneath and the hardness improvements as a result of ion implantation are underestimated. The scatter in the data is greater for tests performed at 5 g load as compared to those performed at the 10 g load, owing to the greater sensitivity of smaller indents to surface imperfections.

Results of friction measurements during fretting wear against stainless steel are shown in Fig. 4. For the dry test condition, the friction levels for the control samples are higher than that of the ion implanted samples. This can also be tied to improved biocompatibility because it is well known that decreased friction is correlated with decreased debris generation as well as reduction in material transfer between the stylus and sample. Additionally, the higher levels of perturbations in the friction curve for the control samples are indicative of greater propensity for ''stick-slip'' type wear behavior in this case. This is caused by micro-adhesion between the two wearing surfaces, a phenomenon commonly termed galling. Galling is reduced as a result of ion implantation, possibly due to a decrease in mutual solubilities of the two wearing surfaces.

The transfer of material due to galling was supported by SEM observations and energy dispersive spectroscopy (EDS) elemental analysis when fretting wear scars were examined with a field emission SEM. As may be noted in the micrographs shown in Fig. 5, the size and the topography of the wear scars are distinctly different for the various sample conditions. SEM examination of the wear scars on implanted and control samples and energy dispersive X-ray spectroscopy (EDS) analysis clearly indicated that the transfer of stainless steel to the Ni–Ti sample was inhibited by ion implantation.

Wear track depths were measured using an Alpha Step 2000 profilometer with a measurement range of $\pm$ 160 μm and reported accuracy of 0.5 nm. A typical series of wear track profiles under lubricated condition is shown in Fig. 6. The wear data summarized in Fig. 7 indicate an improvement in wear behavior for the austenitic samples with a 40% reduction in wear depth between control and ion implanted austenitic samples under dry conditions and a 80% reduction under lubricated conditions. As expected, wear behavior is

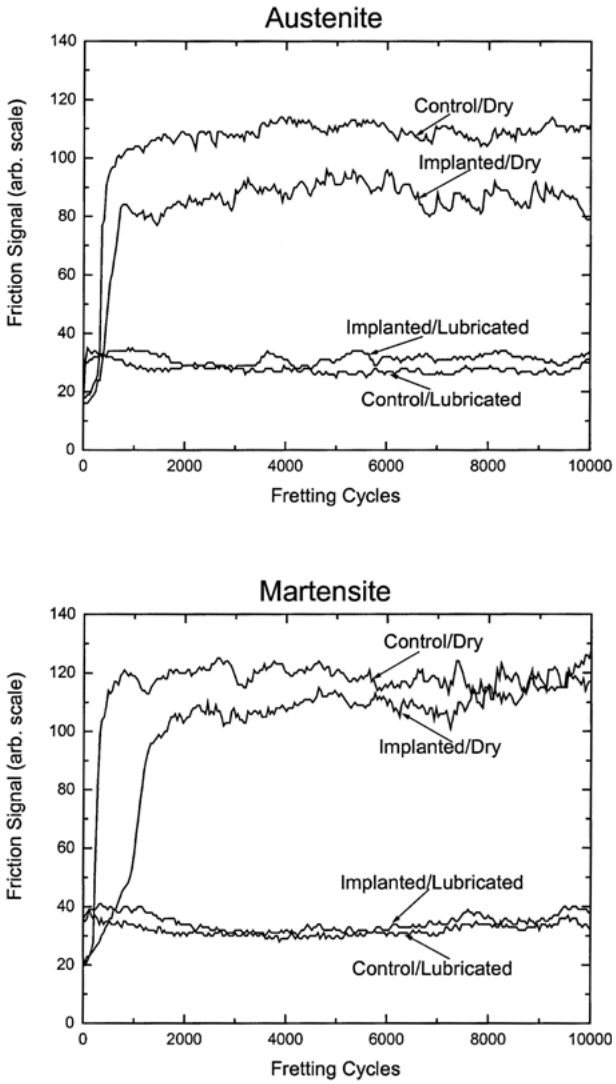

Figure 4 Friction measurements as a function of the number of fretting wear cycles.

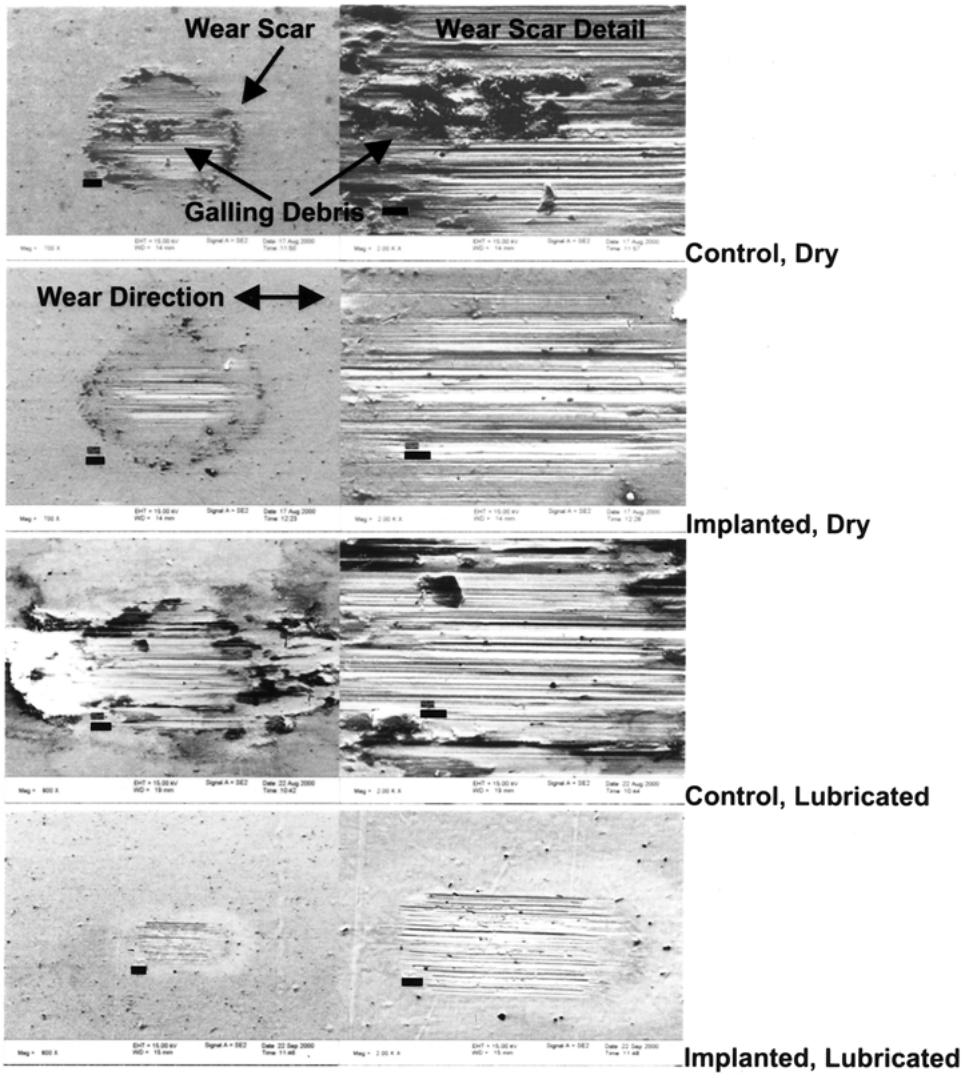

Figure 5 Scanning electron micrographs of Ni–Ti wear surfaces for austenitic samples under dry and lubrication conditions. The scale bar is 20 μm in the low magnification images and 10 μm in the high magnification images.

improved significantly with lubrication for both austenitic and martensitic samples. However, no improvement was observed in the wear behavior of martensitic samples after ion implantation.

Discussion

The results presented above represent a confluence of a number of separate and interdependent factors that influence wear behavior and hardness in shape memory alloys such as Ni–Ti. Factors to be considered in the interpretation of microhardness test measurements include the possibility of stress-induced transformation of austenite to martensite during indentation and the pseudoelastic recovery upon removal of the indenting load. Both these factors would yield higher than expected hardness values, and it is clear from Fig. 3 that ion implantation enhances the near-surface hardness of Ni–Ti.

Making relative comparisons between the austenitic and martensitic samples is more difficult because the material in the austenite phase at room temperature is capable of undergoing stress-induced transformation to martensite due to the high concentration of stress at and in the vicinity of the indentation. The martensite phase has the ability to rearrange its twin structure to accommodate some of the imposed strain under the indentation tip, but only a small amount of recovery is expected upon removal of the indenter. Austenite is, however, expected to display significant pseudoelastic recovery upon removal of the indentation load and the hardness values recorded for this phase are expected to be higher because of this effect. The recovered strain may be a major factor for the differences in hardness observed between austenitic and martensitic samples.

Aside from surface hardness, other factors such as the contact stress, the relative motion of the wearing bodies, lubricant, and temperature are thought to play a significant role in wear behavior. Fig. 4 shows that the friction level and galling are significantly influenced by the presence of a lubricant, which correlates with mass loss as measured by profilometry (Fig. 6). The lubricant, artificial plasma for these experiments, decreases the coefficient of friction and makes the friction signal much lower than that of dry condition. Lubrication changes the friction process from one that is accurately modeled by glide friction to one that is modeled by roll friction. Additionally, the lubricant restricts the access of oxygen

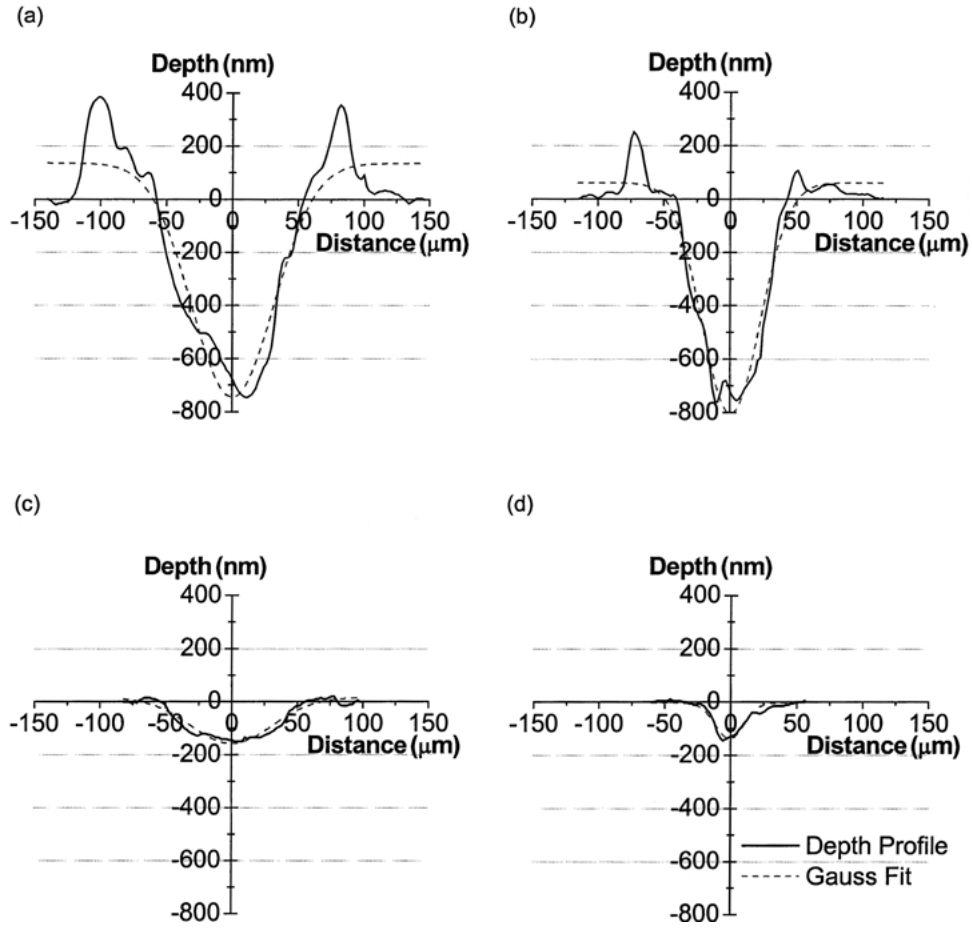

Figure 6 Typical wear track profiles of austenitic samples: (a) control longitudinal direction; (b) control transverse direction; (c) implanted longitudinal direction; (d) implanted transverse direction.

and facilitates heat transfer, which minimize the oxide formation on the surfaces thus decreasing the amount of oxide debris in the wear scar. The lubricant may also facilitate the transfer of fine oxide wear debris to the edges of the wear scar, thereby minimizing the possibility of accelerated three-body wear.

It has been suggested that the high wear resistance of Ni–Ti alloys is a consequence of the material's ability to undergo pseudoelastic transformation under an applied stress [4]. In an appropriate temperature range, the austenite phase of Ni–Ti can undergo pseudoelastic transformation, which allows the material to absorb large strains prior to any permanent deformation. However, if the temperature is below the A_f temperature, the martensite phase of Ni–Ti is present which can only rearrange its twin structure to accommodate some of the imposed strain. It would be reasonable to expect that pseudoelasticity and to a lesser extent, twin rearrangement would at least partially accommodate the high stresses under the stylus. This accommodation would allow the material to resist wear and create less wear debris. If the temperature is too high, however, the material will loose its ability to pseudoelastically transform; deformation beyond the elastic limit is permanent and irreversible.

Because local heating occurs during the wear process, this temperature change must also be taken into account in interpreting the wear results. The austenitic samples have an A_f of 16 °C, whereas the martensitic samples have an A_f of 40 °C as depicted in Fig. 8. Localized heating of the austenite in the wear scar can easily increase the temperature to a level at which pseudoelastic transformation is no longer possible. The temperature range in which pseudoelastic transformation can occur, often called the ''pseudoelastic window'' (shown schematically in Fig. 9), is generally less than 100 °C. The martensitic samples, however, will first transform to the austenitic phase (capable of undergoing pseudoelastic transformation) with the local heating before reaching a temperature high enough to preclude pseudoelastic transformation.

Under dry conditions, the local material has less opportunity to dissipate heat than in lubricated conditions. Thus, the poor wear behavior anticipated because of the lack of lubrication is also exacerbated by the high local temperature at the point of wear which moves the material outside the pseudoelastic window depicted in Fig. 9. With lubrication, the heat developed by friction is more effectively dissipated and the local temperature is lower. The hypothesis that local heating during the wear process moves the temperature outside the pseudoelastic window is supported by the control sample data presented in Fig. 7. Even under lubricated conditions, the local heating in the austenitic sample is sufficient to inhibit pseudoelastic transformation in most of the wear scar. For the martensite control set, this local heating is

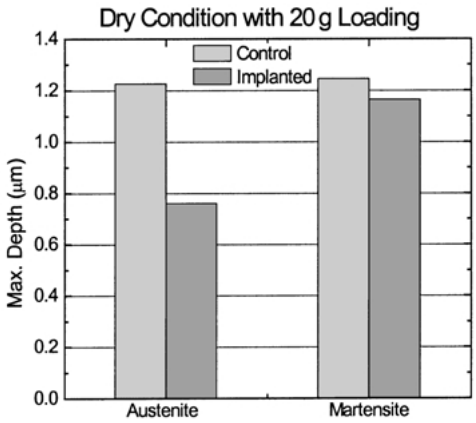

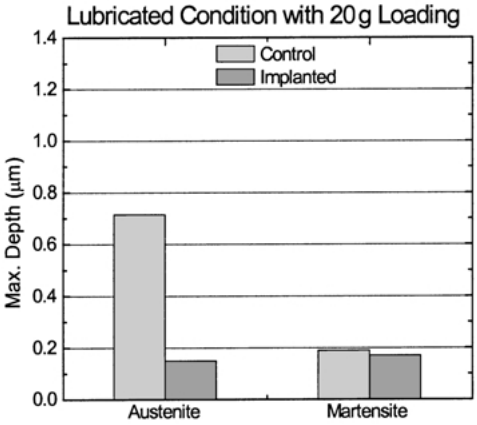

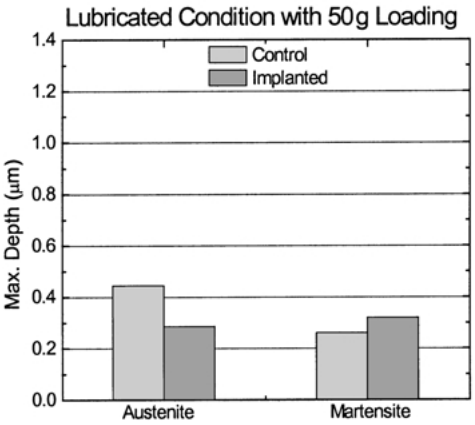

Figure 7 Maximum depth of wear scars for the dry condition with 20 g loading and for the lubricated condition with 20 g and 50 g loading.

beneficial because it moves the material into the pseudoelastic window and dramatically improves the wear resistance.

In the surface modified material, in addition to pseudoelasticity, other factors influence wear behavior. It is well known in the field of tribology that two surfaces in apparent contact are in fact in contact only at a few asperities [27]. Moreover, the volume of wear debris is proportional to the number of asperities in contact [28]. It follows then, that for stronger surfaces fewer asperities will be required to support a given load, thereby resulting in less wear. As evident by the hardness improvements shown in Fig. 3, ion implantation strengthens the

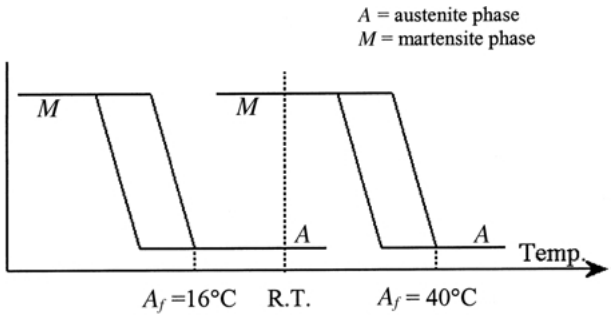

Figure 8 Schematic illustration of the thermal behavior under constant stress. The relative location of the austenitic samples and the martensitic sample is depicted with respect to room temperature.

materials surface, which would translate to less wear. The primary mechanism for improvement in wear resistance in the ion implanted materials is the surface strengthening resulting from the formation of hard, second phase precipitates in the near-surface regions of the materials. In this case, the formation of TiO_2 and to a lesser extent TiC, constitute the primary source of strengthening. The abrasive action of the oxide debris is a factor in fretting corrosion, and therefore the harder the surface, the higher the abrasion resistance, and the less the damage. According to the microindentation hardness results presented earlier, the surface hardness of austenitic samples was significantly increased by PSII modification. This is accompanied by a commensurate improvement in its wear resistance. It should be noted here that the wear behavior of ion implanted Ni–Ti alloy can only be conclusively explained by an understanding of the effect of the implanted species on the stability of the austenite and martensite phases and the magnitude of stress and stress gradient in the implanted layer.

The overall result is that resistance to wear is uniformly improved by the presence of the surface modified layer. Wear behavior is not critically dependent on the local temperature at the wear site and the pseudoelastic window is no longer a factor. Further, the improvement in wear produced by ion implantation is similar to the improvement observed when Ni–Ti is able to pseudoelastically transform.

Conclusion

Fretting wear behavior of Ti–50.8 at % Ni alloy was investigated by comparing the results of control samples and implanted samples under dry and lubrication wear conditions. It was demonstrated that the wear resistance property of Ni–Ti was highly improved by PSII technique without loosing the bulk shape memory effect. Significant improvements in wear resistance were observed in the austenitic samples implanted with argon and oxygen. The maximum depth of the wear scar for the surface modified samples was 40% lower in the dry condition and 80% lower in the lubricated condition when compared to the control samples. It is concluded that both hardness and pseudoelasticity play important roles in the wear resistance of Ni–Ti shape memory alloys.

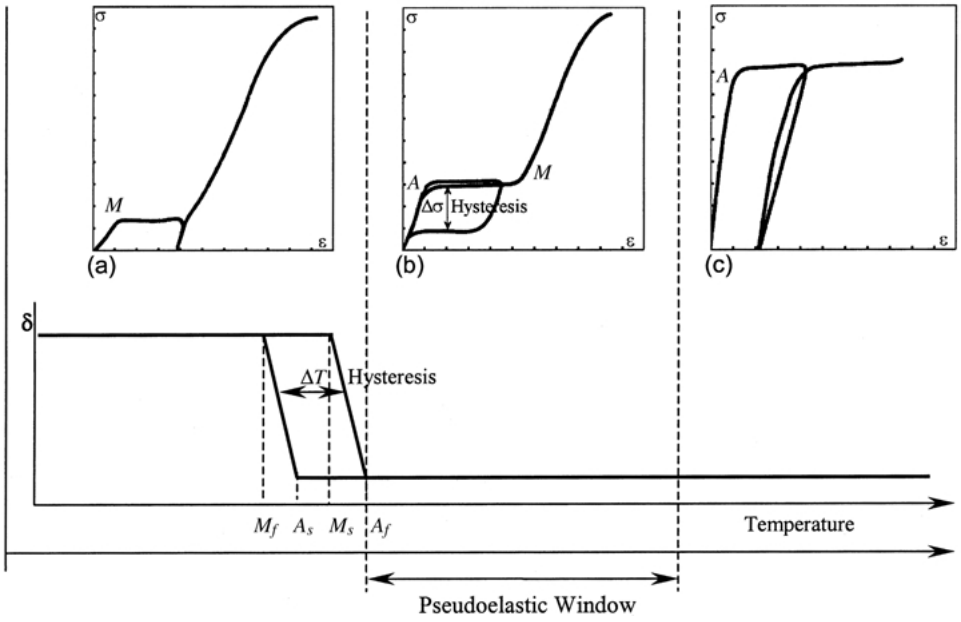

Figure 9 Schematic depiction of the ''pseudoelastic window.'' The three graphs at the top of the figure depict mechanical behavior at three different temperatures (adapted from [9]). The graphs show stress/strain behavior for loading past the elastic limit, followed by unloading, and finally reloading to the ultimate strength of the material. In (a), the strain exhibited after unloading is due to the deformation of the martensite phase (twin rearrangement) and can be recovered by heating above A_f. In (b), the strain is fully recovered after unloading. The temperature range in which this behavior persists is the ''pseudoelastic window.'' Mechanical hystesis between the forward and reverse transformations is identified by $\Delta\sigma$ in figure (b). In (c) the strain exhibited after unloading is non-recoverable plastic strain. The bottom graph depicts thermal behavior under constant stress. This graph shows changes in length (deflection) that occur in a sample with one heating and cooling cycle. Thermal hysteresis between the forward and reverse transformations is identified by ΔT in the bottom graph.

Acknowledgments

Research support for this work was provided by the Whitaker Foundation (RG-99–0201). The authors would also like to thank Erik Wilson, Dan Lawrence, and Buck Johnson for their technical assistance.

References

1. T. W. DUERIG, A. R. PELTON and D. STOCKEL, *Med. Device Diagn. Ind.* March (1997).
2. D. STOECKEL, *Minim. Invasiv. Ther.* **9**(2) (2000) 81.
3. D. Y. LI and R. LIU, *Wear* **225–229** (1999) 777.
4. D. Y. LI, *ibid.* **221** (1998) 116.
5. Y. N. LIANG, S. Z. LI, Y. B. JIN, W. JIN and S. LI, *ibid.* **198** (1996) 236.
6. P. CLAYTON, *ibid.* **162** (1993) 202.
7. J. RYHANEN, *Minim. Invasiv. Ther.* **9**(2) (2000) 99.
8. J. RYHANEN, ''Biocompatibility Evaluation of Nickel-Titanium Shape Memory Metal Alloy,'' Ph.D. Thesis, Oulu University, Finland (1999).
9. C. L. DUNLAP, S. K. VINCENT and B. F. BARKER, *J. Am. Dent. Assoc.* **118** (1989) 449.
10. E. M. H. AL-WAHEIDI, *Quintessence International* **26**(6) (1995) 385.
11. R. VANDENKERCKHOVE, E. TEMMERMAN and R. VERBEECK, *Mater. Sci. Forum*, **289–292** (1998) 1289.
12. M. BERGER-GORBET, B. BROXUP, C. RIVARD and L. H. YAHIA, *J. Biomed. Mater. Res.* **32** (1996) 243.
13. D. J. CHWIRUT, H. S. OKTAY and T. RYAN, in ''SMST-97: Proceedings of the Second International Conference on Shape Memory and Pseudoelastic Technologies'', edited by A. Pelton (Pacific Grove, California, USA, 1997) p. 369.
14. S. TRIGWELL and G. SELVADURAY, in ''SMST-97: Proceedings of the Second International Conference on Shape Memory ad Pseudoelastic Technologies'', edited by A. Pelton (Pacific Grove, California, USA, 1997) p. 383.
15. C.-M. DHAN, S. TRIGWELL and T. W. DUERIG, *Surf. Interface. Anal.* **15** (1990) 349.
16. M. R. WOLFF, Professor of Medicine and Director of Interventional Cardiology, University Hospital and Clinics, University of Wisconsin, Madison, USA, private communication, June 16, 2000.
17. P. MOINE, O. POPOOLA and J. P. VILLAIN, *Scripta Metallurgica* **20** (1986) 305.
18. P. MOINE, O. POPOOLA, J. P. VILLAIN, N. JUNQUA, S. PIMBERT, J. DELAFOND and J. GRILHE, *Surf. Coat. Tech.* **33** (1987) 479.
19. O. POPOOLA, M. F. DENANOT, P. MOINE, J. P. VILLAIN, M. CAHOREAU and J. CAISSO, *Acta Metall.* **37**(3) (1989) 867.
20. J. R. CONRAD, *Mater. Sci. Engr.* A, **116** (1989) 197.
21. A. ANDERS (ed.), ''Handbook of Plasma Immersion Ion Implantation and Deposition'' (John Wiley & Sons, New York, 2000).
22. W. C. CRONE and K. SRIDHARAN, in ''SMST-Proceedings of the International Conference on Shape Memory and Pseudoelastic Technologies'' (2000).
23. G. F. VANDER VOORT and G. M. LUCAS, *Adv. Mater. Process.* **154**(3) (1998) 21.
24. P. W. SANDSTROM, K. SRIDHARAN and J. R. CONRAD, *Wear* **166** (1993) 163.
25. French Association of Standardization (AFNOR), Standard NF S 91–141, September (1990) ISSN 0336-3931.
26. N. MATSUNAMI, Y. YAMAMURA, Y. ITIKAWA, N. ITOH, Y. KAZUMATA, S. MIYAGAWA, K. MORITA and R. SHIMIZU, in ''Energy Dependence of Sputtering Yields of Monoatomic Solids'' (Institute of Plasma Physics, Nagoya University, Chikusa-ku, Nagoya 464, Japan, June 1980).
27. A. D. SARKAR, in ''Wear of Materials'' vol. 18 (Pergamon, Oxford, 1976).
28. J. HALLING (ed.), ''Principals of Tribology'' (Macmillan, London, 1975).
29. A. R. PELTON, J. DICELLO and S. MIYAZAKI, *Minim. Invasiv. Ther.* **9**(2) (2000) 107.

Received 11 April
and accepted 7 September 2001